Proteins in a shear flow

P. Szymczak[a)]
Institute of Theoretical Physics, Warsaw University, ul. Hoza 69, 00-681 Warsaw, Poland

Marek Cieplak
Institute of Physics, Polish Academy of Sciences, Al. Lotnikow 32/46, 02-668 Warsaw, Poland

The conformational dynamics of a single protein molecule in a shear flow is investigated using Brownian dynamics simulations. A structure-based coarse grained model of a protein is used. We consider two proteins, ubiquitin and integrin, and find that at moderate shear rates they unfold through a sequence of metastable states—a pattern which is distinct from a smooth unraveling found in homopolymers. Full unfolding occurs only at very large shear rates. Furthermore, the hydrodynamic interactions between the amino acids are shown to hinder the shear flow unfolding. The characteristics of the unfolding process depend on whether a protein is anchored or not, and if it is, on the choice of an anchoring point. © *2007 American Institute of Physics.*
[DOI: 10.1063/1.2795725]

I. INTRODUCTION

Mechanically induced conformational changes in biomolecules can be accomplished experimentally in many ways. One of them is by using a pulling device, such as an atomic force microscope, another is by involving fluid flow. The pulling device can be used in two basic modes: at a constant pulling velocity or at a constant force. The latter mode results in a nearly homogeneous tension along the backbone of a biomolecule and in an essentially two-state unfolding behavior in simple proteins such as ubiquitin.[1] The flow induced stretching is very different in this respect since—even in the case of the uniform flow—the tension along the backbone increases as one moves from the free end to the tethered end.[2,3] This effect was predicted[4] to lead to emergence of many partially unfolded metastable conformations which arise when one ramps up speeds of flow.

Experiments on flow-generated stretching of biomolecules have been performed either by using the direct bulk flow[5–12] or by using the meniscus forces, for example, in molecular combing[13–16] or the combination of the viscous and meniscus forces, as it is the case in spin-stretching[17,18] technique. The experiments have been usually performed on the long DNA chains. However, in the case of proteins a full unfolding of a molecule requires flow velocities that are three orders of magnitude larger[4] than those needed for the DNA unfolding because of the much smaller hydrodynamic radii and larger intramolecular forces involved. Nevertheless, stretching proteins at smaller flow velocities could still produce interesting effects, since it usually results in the formation of partially unfolded intermediates. However, in contrast to atomic force spectroscopy, there are still no experiments on the protein unfolding in the flow on the single-molecule level. Instead, flow denaturation experiments were carried out on a bulk collection of molecules, usually subject to the shearing forces.[19–23] A notable exception are the studies on

the von Willebrand factor, a large polyprotein found in the blood plasma.[24–26] However, although the existence of shear-induced conformational transition in that system is well documented, it does not seem to involve the unfolding of individual domains of the protein. Instead, a conformational transition of the whole multiunit chain takes place, from a compact globular state to the elongated fiberlike conformation.

The experimental results quoted here seem to suggest that the shear rates needed to unfold a small protein are extraordinarily high. For example, Jaspe and Hagen[23] tried to unfold horse cytochrome with the shear rates as high as 10^5 Hz but observed no evidence of the shear destabilization of the folded state of the protein. They also gave a simple estimate that in order to unfold a protein, the shear rate should be characterized by the Weissenberg number Wi $= st_{\text{fold}}$ of the order of 10^3. Here t_{fold} is the folding time of a protein and s is the shear rate. We confirm that prediction through molecular dynamics simulations of a protein using a coarse-grained model. Additionally, we show that stretching of proteins by shear flow proceeds differently from that of homopolymers.

The simulations were conducted for ubiquitin and integrin. Both have been the subject of our previous investigations on protein stretching in uniform flow. In particular, integrin was shown to possess a surprisingly rich spectrum of metastable states when stretched by the flow[4] which makes it a perfect system in which to investigate the effects of the shear flow.

II. THE MODEL

Coarse-grained models of proteins allow one to access time scales which are orders of magnitude longer than those available in all-atom simulations. Among the coarse-grained models, the Go-like implementations[27,28] link the properties of a protein directly to its native geometry and are probably the easiest to use. We follow the implementation presented in

---

a)Electronic mail: piotrek@fuw.edu.pl

    127, 155106-1

Refs. 29–33. The protein is represented by a chain of its C^α atoms. The successive C^α atoms along the backbone are tethered by harmonic potentials with a minimum at 3.8 Å. The effective interactions between the residues are split into two classes: native and non-native. This determination is made by checking for native overlaps between the enlarged van der Waals surfaces of the amino acids as proposed in Ref. 34. The amino acids, i and j, that do overlap in this sense are endowed with the effective Lennard-Jones potential V_{ij} $=4\epsilon[(\sigma_{ij}/r_{ij})^{12}-(\sigma_{ij}/r_{ij})^6]$. The length parameters σ_{ij} are chosen so that the potential minima correspond, pair by pair, to the experimentally established native distances between the respective amino acids in the native state. Non-native contacts are represented by hard core repulsion in order to prevent entanglements. Another term in the Hamiltonian imposes local stiffness on the backbone. This can be accomplished either by introducing biases in the bond and dihedral angles[35] or by favoring native senses of local chiralities.[36] Here, we choose the latter.

The protein was subject to a simple shear flow of the form

$$v_x = sy, \quad v_y = v_z = 0, \tag{1}$$

which may also be written as $\mathbf{v}=\mathbf{K}\cdot\mathbf{r}$ where K is the velocity gradient matrix, in this case given by

$$K = \begin{pmatrix} 0 & s & 0 \\ 0 & 0 & 0 \\ 0 & 0 & 0 \end{pmatrix}. \tag{2}$$

In our previous studies on uniform flow unfolding[4] we used the Langevin dynamics method to track the evolution of the system. Here, however, we use the Brownian dynamics scheme since it allows for a straightforward incorporation of hydrodynamic interactions (HI). Without the hydrodynamic interactions, the two schemes (Langevin and Brownian dynamics) give the same results, since on the time scales characteristic for protein unfolding, the motion is overdamped and inertia effects are negligible, as confirmed in Ref. 37.

In the Brownian dynamics algorithm,[38] the displacement of the ith amino acid during the time step Δt is given by

$$\Delta\mathbf{r}_i = \mathbf{K}\cdot\mathbf{r}_i\Delta t + \sum_j (\nabla_j\cdot\mathbf{D}_{ij})\Delta t + \frac{1}{k_BT}\sum_j \mathbf{D}_{ij}\cdot\mathbf{F}_j\Delta t$$
$$+ \mathbf{C}_i{:}\mathbf{K}\Delta t + \mathbf{B}_i. \tag{3}$$

Here $\mathbf{r}_i$ is the position of ith amino acid, $\mathbf{F}_i$ is the total interparticle force acting on it, and $\mathbf{D}$ is the diffusion tensor. Note that both $\mathbf{F}$ and $\mathbf{D}$ are configuration dependent. Next, $\mathbf{B}$ is a random displacement given by a Gaussian distribution with an average value of zero and covariance obeying

$$\langle\mathbf{B}_i\mathbf{B}_j\rangle = 2\mathbf{D}_{ij}\Delta t. \tag{4}$$

Finally, $\mathbf{C}$ is the third rank shear disturbance tensor[39] representing the effect of interparticle hydrodynamic forces on the shear-induced particle motion.[40,41] Most of our simulations were conducted without taking hydrodynamic interactions into account (free draining model). In this case, the diffusion tensor is diagonal,
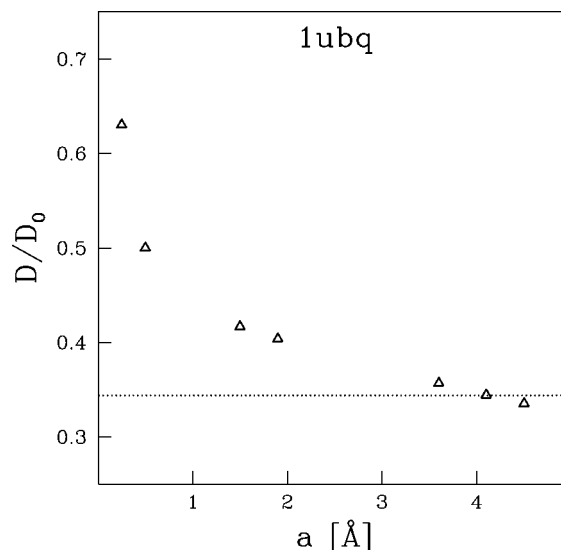

FIG. 1. Reduced diffusion coefficient as a function of a hydrodynamic radius of an amino acid. The horizontal line marks the experimental value $D/D_0 \approx 0.345$.

$$\mathbf{D}_{ij} = \frac{k_BT}{6\pi\eta a}\mathbf{I}\delta_{ij}, \tag{5}$$

and the disturbance matrix vanishes. At the end of the paper, we discuss the influence of the hydrodynamic interactions on the mean extension at various shear rates. In that case, we use the approximation of Rotne and Prager,[42] and Yamakawa[43] of the diffusion tensor, with the nondiagonal terms of $\mathbf{D}_{ij}$ given by

$$\mathbf{D}_{ij} = \frac{k_BT}{8\pi\eta r_{ij}} \begin{cases} \left[\left(1+\frac{2a^2}{3r_{ij}^2}\right)\mathbf{I}+\left(1-\frac{2a^2}{r_{ij}^2}\right)\hat{\mathbf{r}}_{ij}\hat{\mathbf{r}}_{ij}\right], & r_{ij}\geqslant 2a \\ \frac{r_{ij}}{2a}\left[\left(\frac{8}{3}-\frac{3r_{ij}}{4a}\right)\mathbf{I}+\frac{r_{ij}}{4a}\hat{\mathbf{r}}_{ij}\hat{\mathbf{r}}_{ij}\right], & r_{ij} < 2a \end{cases} \tag{6}$$

where $\mathbf{r}_{ij}=\mathbf{r}_j-\mathbf{r}_i$ and a represents the hydrodynamic radius of a bead.

When taking the hydrodynamic interactions into account, the choice of a hydrodynamic radius, a, is a crucial element in the model. One of the ways of tuning this parameter is to compare the translational diffusion coefficient D, of a protein in a numerical model, to the one measured in experiment. Figure 1 shows the dependence of $D'=D/D_0$ on the hydrodynamic radius. Here the diffusion coefficients D are normalized by $D_0=kT/6\pi\eta R$, the diffusion coefficient of the bead of radius $R=5$ Å. In water at $T=300$ K, with viscosity of $\eta=0.89\times10^{-2}$ P, one gets $D_0=4.93\times10^{-6}$ cm^2/s. The experiment[44] gives the diffusion coefficient of ubiquitin $D=1.7\times10^{-6}$ cm^2/s, or, equivalently, $D'=0.345$. As can be seen from the data, the agreement with experiment is obtained for $a\approx4.1$. This value agrees with earlier estimates by de la Torre et al.,[45,48] Antosiewicz and Porschke,[46] Hellweg et al.,[47] and Banachowicz et al.[49] However, since the distance between the successive C^α atoms along the protein backbone is 3.8 Å, some of the beads representing amino acids overlap. This reflects the fact that (1) the interior of the

protein is densely packed, (2) the side chains of amino acids are usually longer than 3.8 Å, and (3) the protein is covered by the hydration layer of tightly bound water molecules. Although the Rotne-Prager tensor is positive definite also for overlapping beads, its physical meaning for such configurations is problematic.[48] The overlapping bead models are successful in predicting the diffusion coefficients of the proteins,[45,46] however, the question whether they correctly reproduce the dynamic effects of hydrodynamic interactions during large-scale conformational motions in macromolecules is still open. To investigate the influence of the hydrodynamic radius on the dynamics of the protein in the flow, we compare the results obtained for $a=4.1$ with those for a smaller value of the hydrodynamic radius, $a=1.5$ Å. The analysis of Fig. 1 shows that the choice of $a=1.5$ Å overestimates the diffusion coefficients by 20% only, but has the advantage of not leading to overlapping configurations of the spheres with the radii of a. Such a value of a was also used in our previous studies on the influence of hydrodynamic interactions on protein unfolding[37] whereas Baumketner and Hiwatari[50] use $a=1.77$ in their investigations on the influence of HI on the protein folding process.

A natural time scale in the simulations, τ, is set by the time it takes for the amino acid (i.e., the object of the radius $a=4.1$ Å) to diffuse the distance of its radius, a. Again, in water at $T=300$ K, one gets $\tau=0.05$ ns. This time scale is used as a time unit in the data reported, irrespective of the actual value of hydrodynamic radius used (4.1 or 1.5 Å).

The folding time for ubiquitin, as calculated according to the scheme described, e.g., in Ref. 30 in the free-draining case (with $a=4.1$ Å) is equal to $t_{\text{fold}} \approx 1100\tau$ whereas for integrin $t_{\text{fold}} \approx 8000\tau$. When the hydrodynamic interactions are taken into account ubiquitin folding time becomes $t_{\text{fold}} \approx 370\tau$ for $a=4.1$ and $t_{\text{fold}} \approx 150\tau$ for $a=1.5$. The latter difference is caused mainly by the differences in the single amino acid diffusion coefficients in both cases; the ratio of the diffusion coefficients $(4.1/1.5) \approx 2.7$ is only about 10% larger than the corresponding ratio of folding times, $(370/150) \approx 2.5$.

The initial conformation of the protein corresponds to the native structure. During the simulations either one of the termini of the protein is anchored or both ends are free. In both cases, the fluid in which the protein is immersed is unbounded in all directions The end-to-end extension, the orientation angle, and the root-mean-square derivation (RMSD) from the native structure are then recorded as a function of time. The total length of the simulation time for each trajectory was $t=400\,000\tau$ for the free-draining case (for both ubiquitin and integrin) and $t=10\,000\tau$ for the simulations with hydrodynamic interactions (for ubiquitin). The nondimensional flow strength is characterized by the Weissenberg number, $\text{Wi}=s\tau_0$, where, following Jaspe and Hagen,[23] we take τ_0 to be equal to the folding time of the protein, t_{fold}.

III. RESULTS

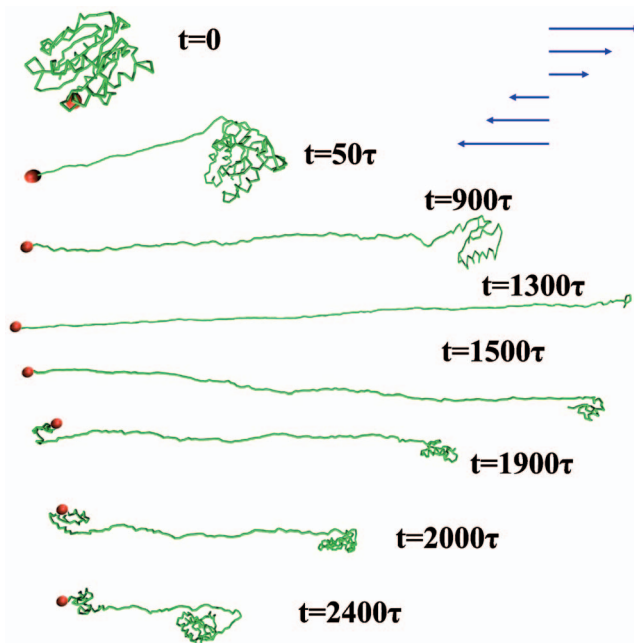As already noted by Lumley[51] and de Gennes,[52] a notable feature of the shear flow is that it is a combination of

FIG. 2. (Color) Example of cycle of the motion of a tethered protein in shear flow: integrin at $s=0.25\tau^{-1}$ (Wi=2000). The anchoring point (C terminus) is marked by a circle.

the elongational and rotational components of equal magnitudes. In such a marginal case the polymer chain does not attain a stable stretched configuration. Instead, it undergoes a tumbling motion, a series of subsequent stretching and coiling events with frequent changes in the orientation of the chain with respect to the shear axis.[7–10] While the elongational component of the flow is stretching the molecule, its rotational component aligns it along the shear axis, leading to the collapse of the chain due to the decreased hydrodynamic drag. An important role in this dynamics is played by the Brownian fluctuations, which cause the chain segments to cross the streamlines into the regions of higher or lower flow which results in further stretching or collapse of the chain, respectively. In particular, the fluctuations may tip the polymer in such a way that its two ends lie in the regions of opposite flow direction, which results in a tumbling event, in which one polymer end moves over the other.

We show that the tumbling dynamics are also seen in the case of protein stretching by a shear flow. As an example, Figs. 2 and 3 show the time series of configurations of intergrin in shear flow for both tethered and free protein. However, the presence of a complex network of bonds between amino acids in a protein results in a number of important differences between the homopolymer and protein unfolding. In particular, the extension of the protein in the uniform flow is not a continuous function of the flow rate. Instead, as the flow velocity is increased, the protein undergoes a number of rapid transitions to the successive metastable states. Each of those transitions is accompanied by the breaking of a particular group of bonds and unzipping of subsequent structures from the bulk of the protein. As an example, Fig. 4 shows the set of intermediates arising during unfolding of the integrin molecule in a uniform flow.

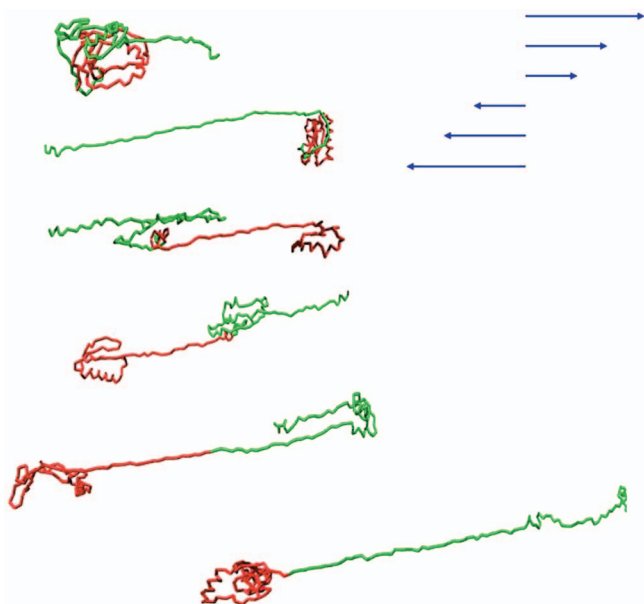The presence of intermediate states is also observed in

FIG. 3. (Color) Example of cycle of the motion of a free protein in shear flow: integrin at $s=0.4\tau^{-1}$ (Wi=3200). For tracing purposes, half of the chain is colored red, and another half is colored green.

the case of the shear flow. However, in a shear flow those states are never long lived, even a small thermal fluctuation may move the protein to the region of smaller flow and the molecule collapses. Nevertheless, some fingerprints of the underlying discrete set of intermediate states are present even in the histogram of end-to-end distances, which shows the maxima corresponding to the metastable states observed in the uniform flow stretching. As an example, Fig. 4 shows the end-to-end length distribution for the integrin molecule teth-
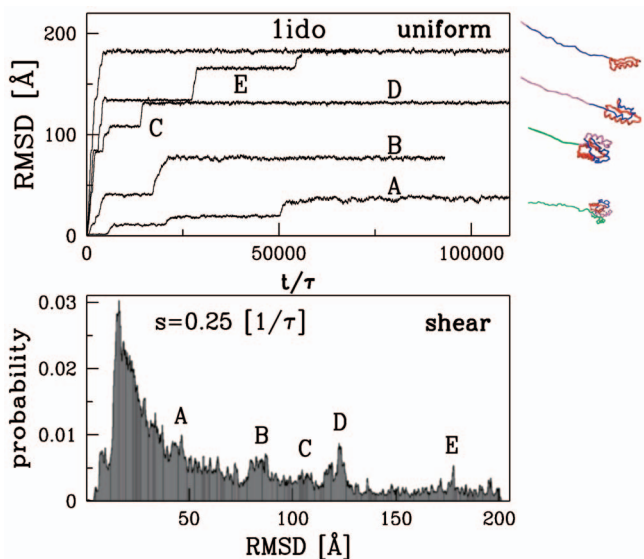

FIG. 4. (Color) Integrin tethered by the C terminus. (Upper) Examples of the time evolution of the RMSD from the native structure in unfolding of integrin in a uniform flow for various flow rates. The plateaus correspond to successive stationary conformations (intermediates) marked by the letters (A)–(E). The snapshots of conformations A, B, D, and E are shown on the right. (Lower) The histogram of RMSD for the integrin in a shear flow at Wi=2000. The respective values of RMSD corresponding to the intermediates seen in the upper panel are marked.
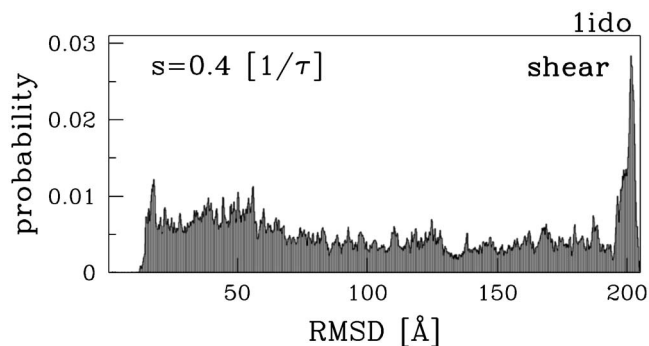

FIG. 5. Same as in the lower panel of Fig. 4 but for $s=0.4\tau^{-1}$ (Wi=3200).

ered by the C terminus. Such a peak structure in the histogram is observed for medium shear rates only; lower shear rates are not strong enough for the intermediates to overcome the free energy barrier needed to partially unfold the chain whereas in the case of high shear rates the tumbling rate increases, the protein spends even less time in the stationary conformations and thus the histogram no longer shows the intermediates. Figure 5 gives an example of the end-to-end length distribution for the 50% higher shear rate than that in Fig. 4. As it is seen, the peak structure is now almost impossible to discern.

It is worth noting that in the case of homopolymer in a shear flow, the respective probability distributions have a much simpler structure. As an example, Fig. 6 shows the RMSD histogram for a simple helix (of 48 residues) in a shear flow. Also the histograms of the chain extension in DNA experiments are usually much smoother, with one or two maxima only.[11]

The characteristics of uniform flow unfolding are asymmetric with respect to the protein anchoring.[4] For example, integrin unfolds more easily when tethered by the C terminus. Also, the C terminus tethering leads to a much richer spectrum of intermediates than the N terminus tethering. As mentioned in the introduction, this asymmetry is caused by the fact that the tension along the protein backbone increases from the free end towards the tethered one when the molecule is placed in the flow. Such an asymmetry can also be seen in the shear flow unfolding. In particular, Fig. 7 shows the relative extension (L/L_0) of the integrin molecule as a function of the Weissenberg number for different tethering points. Here the average end-to-end distance of the molecule
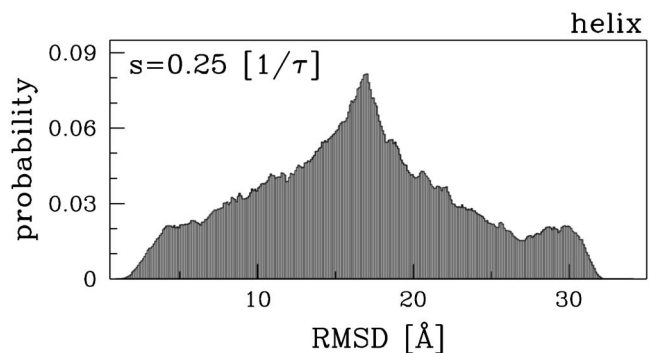

FIG. 6. Histogram of RMSD for the helix (48 residues) in a shear flow at $s=0.25/\tau$.
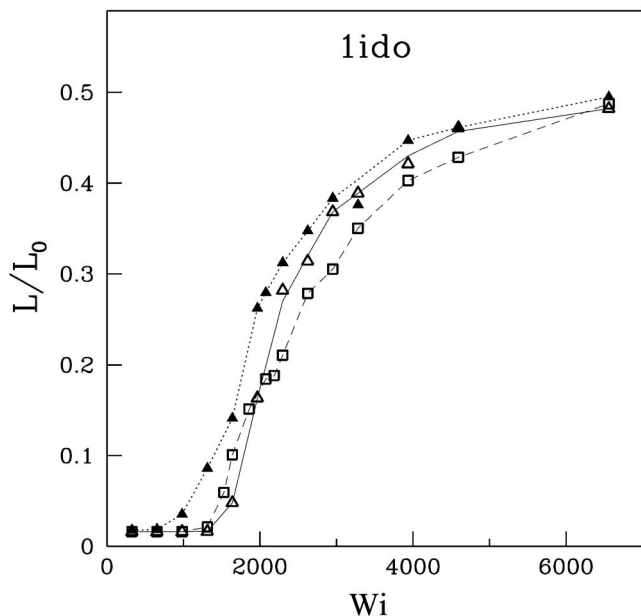
FIG. 7. Relative extension of the integrin molecule as a function of the Weissenberg number for a chain tethered by the C terminus (filled triangles), N terminus (empty triangles), and a free chain (squares). The average end-to-end distance of the molecule (L) is normalized by the maximum extension length $L_0 = (N-1) \times 3.8$ Å, where N is the number of amino acids.

FIG. 8. Power spectral density (psd) of the protein orientation angle for integrin tethered by the N terminus in a shear flow at Wi=1600. Frequencies are scaled by the protein folding time and the psd is normalized with its maximum value.

(L) is normalized by the maximum extension length $L_0 = (N-1) \times 3.8$ Å, where N is the number of amino acids. It is seen that the C terminus tethering allows unfolding at a lower shear rate, which is consistent with the uniform flow stretching results. The critical shear rate, at which the unfolding events begin to take place is shifted from Wi=600 in the case of the C terminus tethering to about Wi=1300 for the N terminus tethering. Finally, when both ends of a protein are free, the critical shear rate is the same as in the N tethering case (Wi=1300), but the shape of the dependence of L/L_0 on Wi is slightly different from that observed for the N tethering.

As noted by Smith et al.[7] and Doyle et al.,[8] the power spectral density of the end-to-end polymer extension in a shear flow shows no distinct peaks which indicates that no periodicity is present in the evolution of this variable. However, it was subsequently reported[10,53] that there are other variables characterizing the polymer motion which show the periodic behavior. In particular, a well defined characteristic tumbling frequency is revealed in the spectrum of a polymer orientation angle θ.[10] Analogous spectrum for the protein is presented in Fig. 8. Two peaks can be identified in the spectrum, corresponding to two characteristic tumbling frequencies. The higher frequency is the one associated with the rotational component of the shear flow, $f_1 = s/4\pi$ [a sphere immersed in the shear field rotates with the frequency f_1 (Ref. 39)]. On the other hand, the lower frequency, f_2, corresponds to the stretching-collapse cycle and scales sublinearly with the flow rate, similar to what was reported in DNA experiments.[10] Both dynamical behaviors are observed in Fig. 9 which shows the time trace of the protein orientation angle and the associated evolution of the RMSD. In the high frequency regime, the protein is closely packed, with small
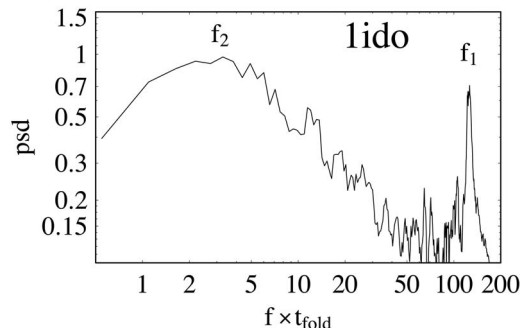
values of RMSD away form the native structure and it essentially behaves like a sphere rotating in a shear flow. From time to time, a sudden unfolding event takes place—the protein ceases to rotate and its RMSD rapidly increases. For larger shear rates, the unfolding events are more frequent and the periods of free rotation in the globular state—shorter, as seen in Fig. 10. Figure 11 shows the tumbling frequencies f_1 and f_2 as the function of Wi. Note that there is a relatively narrow shear rate range for which both frequencies are visible in the spectrum. For lower shear rates the protein hardly ever unfolds hence f_2 is impossible to discern. On the other hand, at large shear rates the protein is never found in a globular state for a sufficient period of time for f_1 to be seen.

The inclusion of hydrodynamic interactions considerably hinders the unfolding of a molecule. Figure 12 shows the comparison of the relative extension of ubiquitin in a shear flow calculated with and without the hydrodynamic interactions. It is seen that, when HI are included in the model, much larger shear rates are needed for the unfolding of a
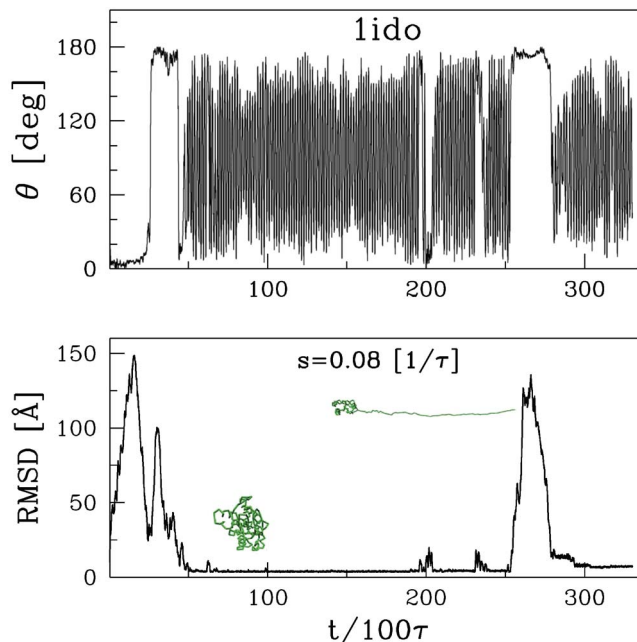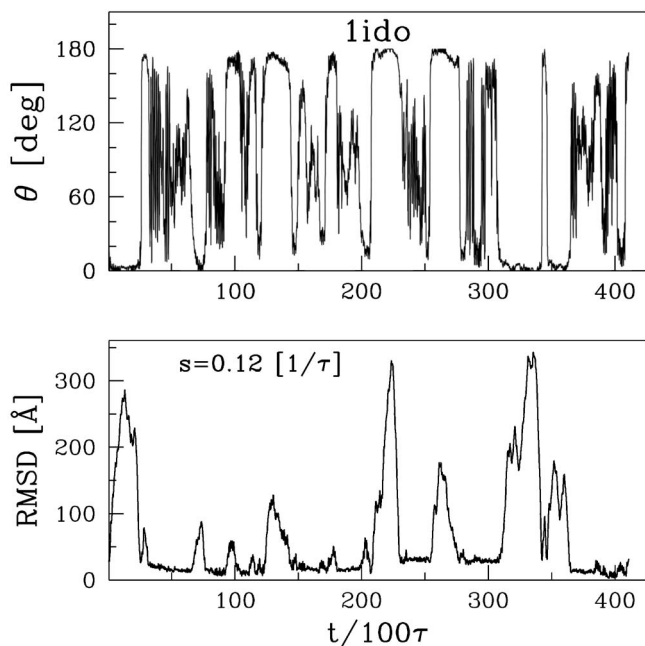

FIG. 9. (Color online) Angle θ between the end-to-end direction of the protein and the direction of the flow (upper panel) and RMSD for integrin tethered by the C terminus in a shear flow at Wi=640 (lower panel).

FIG. 10. Same as in Fig. 9 but for Wi=960

molecule and the corresponding extensions of the chain are significantly smaller. In particular, a critical shear rate needed for the unfolding events to take place is shifted from Wi=250 for the non-HI case to Wi=600 (HI present, a=1.5) and Wi=2000 (HI present, a=4.1). This is consistent with our earlier studies on the uniform flow unfolding[37] where it was observed that unfolding of the system with HI requires a much larger flow speed than without. This tendency can be understood qualitatively in terms of the so-called nondraining effect:[54] the residues hidden inside the protein are shielded from the flow and thus only a small
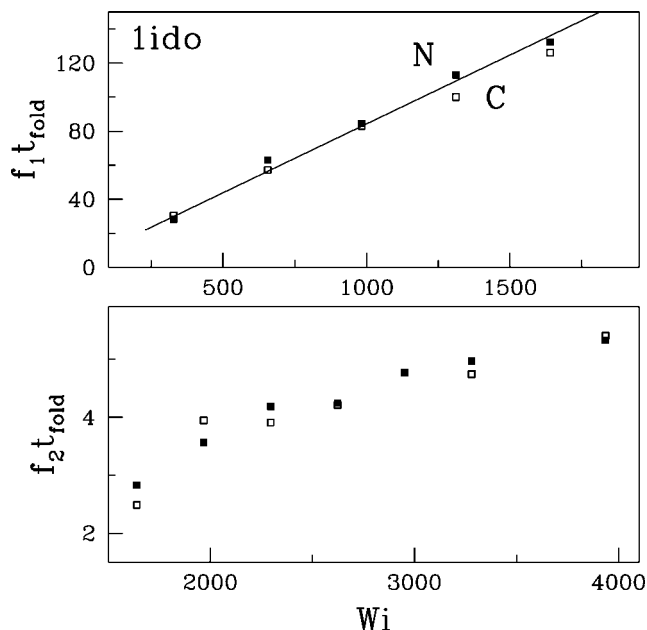

FIG. 11. Peak frequencies f_1 and f_2 derived from the power spectrum densities of orientation angle as a function of the Weissenberg number for integrin tethered by the C terminus (empty squares) and the N terminus (filled squares). The solid line corresponds to the relation $f_1 = s/4\pi$.
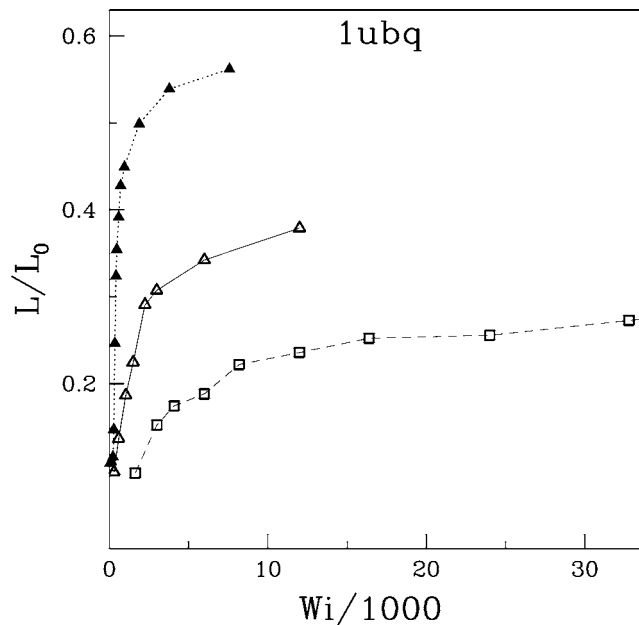

FIG. 12. Relative extension of ubiquitin anchored by the N terminus as a function of the Weissenberg number for the model without hydrodynamic interactions (filled triangles), and with hydrodynamic interactions for a=1.5 Å (open triangles) and a=4.1 Å (squares).

fraction of the residues experience the full drag force of $F = -\gamma U$. In contrast, when no HI are present, this drag force is applied to all residues. This effect is analyzed more quantitatively e.g., in Ref. 55 where, in particular, it is shown that the hydrodynamic shielding increases with an increase in both the hydrodynamic radius and the total number of beads in the polymer chain.

IV. SUMMARY

We have presented Brownian dynamics simulation results on the conformational dynamics of individual protein molecules in the flow. The presence of a network of bonds between amino acids in a protein leads to a number of important differences between the homopolymer and protein unfolding. In particular, in the case of proteins, the characteristics of the unfolding process are shown to depend on the selection of the point of anchor. Additionally, for moderate shear rates, a number of intermediate stages in the unfolding may be discerned, with well defined RMSD values with respect to the native structure. Full unfolding of the proteins was found to occur only at very high shear rates, which is consistent with the experimental results.[23]

ACKNOWLEDGMENTS

[1] M. Schlierf, H. Li, and J. M. Fernandez, Proc. Natl. Acad. Sci. U.S.A. **101**, 7299 (2004).

[2] J. F. Marko and E. D. Siggia, Macromolecules **28**, 8759 (1995).

[3] R. Rzehak, W. Kromen, T. Kawakatsu, and W. Zimmermann, Eur. Phys. J. E **2**, 3 (2000).

[4] P. Szymczak and M. Cieplak, J. Chem. Phys. **125**, 164903 (2006).

[5] T. T. Perkins, D. E. Smith, R. G. Larson, and S. Chu, Science **268**, 83 (1995).

[6] R. G. Larson, T. T. Perkins, D. E. Smith, and S. Chu, Phys. Rev. E **55**, 1794 (1997).

[7] D. E. Smith, H. P. Babcock, and S. Chu, Science **283**, 1724 (1999).

[8] P. S. Doyle, B. Ladoux, and J.-L. Viovy, Phys. Rev. Lett. **84**, 4769 (2000).

[9] R. Teixeira, H. Babcock, E. Shaqfeh, and S. Chu, Macromolecules **38**, 581 (2005).

[10] C. M. Schroeder, R. E. Teixeira, E. S. Shaqfeh, and S. Chu, Phys. Rev. Lett. **95**, 018301 (2005).

[11] C. Schroeder, R. Teixeira, E. Shaqfeh, and S. Chu, Macromolecules **38**, 1967 (2005).

[12] E. S. G. Shaqfeh, J. Non-Newtonian Fluid Mech. **130**, 1 (2005).

[13] T. R. Strick, M. Dessinges, G. Charvin, N. H. Dekker, J. Allemand, D. Bensimon, and V. Croquette, Rep. Prog. Phys. **66**, 1 (2003).

[14] X. Michalet, R. Ekong, F. Fougerousse, S. Rousseaux, C. Schurra, N. Hornigold, M. Van Slegtenhorst, J. Wolfe, S. Povey, J. S. Beckmann, and A. Bensimon, Science **277**, 1518 (1997).

[15] O. B. Bakajin, T. A. J. Duke, C. F. Chou, S. S. Chan, R. H. Austin, and E. C. Cox, Phys. Rev. Lett. **80**, 2737 (1998).

[16] P. Björk, A. Herland, I. G. Scheblykin, and O. Inganäs, Nano Lett. **5**, 1948 (2005).

[17] H. Yokota, J. Sunwoo, M. Sarikaya, G. van den Engh, and R. Aebersold, Anal. Chem. **71**, 4418 (1999).

[18] J. Kim, W.-X. Shi, and R. Larson, Langmuir **23**, 755 (2007).

[19] S. E. Charm and B. Low Wong, Science **170**, 466 (1970).

[20] C. R. Thomas, A. W. Nienow, and P. Dunhill, Biotechnol. Bioeng. **21**, 2263 (1979).

[21] C. R. Thomas and P. Dunhill, Biotechnol. Bioeng. **21**, 2279 (1979).

[22] Y. F. Maa and C. C. Hsu, Biotechnol. Bioeng. **51**, 458 (1996).

[23] J. Jaspe and S. J. Hagen, Biophys. J. **91**, 3415 (2006).

[24] A. Alexander-Katz, M. F. Schneider, S. W. Schneider, A. Wixforth, and R. R. Netz, Phys. Rev. Lett. **97**, 138101 (2006).

[25] S. W. Schneider, S. Nuschele, A. Wixforth, C. Gorzelanny, A. Alexander-Katz, R. R. Netz, and M. F. Schneider, Proc. Natl. Acad. Sci. U.S.A. **104**, 7899 (2007).

[26] C. A. Siedlecki, B. J. Lestini, K. Kottke-Marchant, S. J. Eppel, and D. L. Wilson, Blood **88**, 2939 (1996).

[27] H. Abe and N. Go, Biopolymers **20**, 1013 (1981).

[28] S. Takada, Proc. Natl. Acad. Sci. U.S.A. **96**, 11698 (1999).

[29] T. X. Hoang and M. Cieplak, J. Chem. Phys. **112**, 6851 (2000).

[30] T. X. Hoang and M. Cieplak, J. Chem. Phys. **113**, 8319 (2000).

[31] M. Cieplak and T. X. Hoang, Biophys. J. **84**, 475 (2003).

[32] M. Cieplak, T. X. Hoang, and M. O. Robbins, Proteins: Struct., Funct., Bioinf. **56**, 285 (2003).

[33] J. I. Sułkowska and M. Cieplak, J. Phys.: Condens. Matter **19**, 283201 (2007).

[34] J. Tsai, R. Taylor, C. Chotchia, and M. Gerstein, J. Mol. Biol. **290**, 253 (1999).

[35] C. Clementi, H. Nymeyer, and J. N. Onuchic, J. Mol. Biol. **298**, 937 (2000).

[36] J. I. Kwiecinska and M. Cieplak, J. Phys.: Condens. Matter **17**, 1565 (2005).

[37] P. Szymczak and M. Cieplak, J. Phys.: Condens. Matter **19**, 258224 (2007).

[38] D. L. Ermak and J. A. McCammon, J. Chem. Phys. **69**, 1352 (1978).

[39] J. G. Dhont, *An Introduction to Dynamics of Colloids* (Elsevier, Amsterdam, 1996).

[40] P. Mazur and W. van Saarlos, Physica A **115**, 21 (1982).

[41] M. C. Bujan-Nunez and E. Dickinson, J. Chem. Soc., Faraday Trans. **90**, 2737 (1994).

[42] J. Rotne and S. Prager, J. Chem. Phys. **50**, 4831 (1969).

[43] H. Yamakawa, J. Chem. Phys. **53**, 436 (1970).

[44] A. J. Dingley, J. P. Mackay, G. L. Shaw, B. D. Hambly, and G. F. King, J. Biomol. NMR **10**, 1 (1997).

[45] J. Garcia de la Torre and V. A. Bloomfield, Q. Rev. Biophys. **14**, 81 (1981).

[46] J. Antosiewicz and D. Porschke, J. Phys. Chem. **93**, 5301 (1989).

[47] T. Hellweg, W. Eimer, E. Krahn, K. Schneider, and A. Muller, Biochim. Biophys. Acta **1337**, 311 (1997).

[48] J. Garcia De La Torre, M. L. Huertas, and B. Carrasco, Biophys. J. **78**, 719 (2000).

[49] E. Banachowicz, J. Gapinski, and A. Patkowski, Biophys. J. **78**, 70 (2000).

[50] A. Baumketner and Y. Hiwatari, J. Phys. Soc. Jpn. **71**, 3069 (2002).

[51] J. Lumley, Annu. Rev. Fluid Mech. **1**, 367 (1969).

[52] P. G. de Gennes, J. Chem. Phys. **60**, 5030 (1974).

[53] R. Delgado-Buscalioni, Phys. Rev. Lett. **96**, 1 (2006).

[54] R. Rzehak, W. Kromen, T. Kawakatsu, and W. Zimmermann, Eur. Phys. J. E **2**, 3 (2000).

[55] U. S. Agarwal and R. A. Mashelkar, J. Chem. Phys. **100**, 6055 (1994).